Hindawi
Advances in Condensed Matter Physics
Volume 2018, Article ID 9324528, 9 pages
https://doi.org/10.1155/2018/9324528

Review Article

Progress on Waveguide-Integrated Graphene Optoelectronics

Jiaqi Wang[1,2,3] **Zhenzhou Cheng**[4] **and Xuejin Li**[1,2,3]

[1]*College of Physics and Energy, Shenzhen University, Shenzhen 518060, China*
[2]*Shenzhen Key Laboratory of Sensor Technology, Shenzhen 518060, China*
[3]*Shenzhen Engineering Laboratory for Optical Fiber Sensors and Networks, Shenzhen 518060, China*
[4]*Department of Chemistry, The University of Tokyo, Tokyo 113-0033, Japan*

Correspondence should be addressed to Xuejin Li; lixuejin@szu.edu.cn

Received 13 March 2018; Accepted 18 April 2018; Published 20 May 2018

Academic Editor: Jörg Fink

Graphene, a single layer of carbon atoms arranged in the form of hexagonal lattice, has many intriguing optical and electrical properties. However, due to the atomic layer thickness, light-matter interactions in the monolayer graphene are naturally weak when the light is normally incident to the material. To overcome this challenge, waveguide-integrated graphene optoelectronic devices have been proposed and demonstrated. In such coplanar configurations, the propagating light in the waveguide can significantly interact with the graphene layer integrated on the surface of the waveguide. The combination of photonic integrated circuits and graphene also enables the development of graphene devices by using silicon photonic technology, which greatly extends the scope of graphene's application. Moreover, the waveguide-integrated graphene devices are fully CMOS-compatible, which makes it possible to achieve low-cost and high-density integration in the future. As a result, the area has been attracting more and more attention in recent years. In this paper, we introduce basic principles and research advances of waveguide-integrated graphene optoelectronics.

1. Introduction

Graphene, a two-dimensional (2D) material, has unique features of energy band structure involving zero band gap [1], linear dispersion [2], and low density of states [3–6], which result in intriguing optical and electrical properties and bring us many promising applications. For example, graphene has a linear and gapless energy band diagram, which make it suitable for the development of broadband saturable absorbers (SAs) in passive mode-locked ultrafast lasers [7, 8]. Moreover, graphene-based SAs are easier to be fabricated, comparing to traditional semiconductor SAs and single-wall nanotube SAs which require precise bandgap engineering during fabrication processes. Combing with the feature of high electron mobility, graphene can be used to develop broadband and high-speed photodetectors [9]. However, it is practically difficult to demonstrate such optoelectronic devices with high efficiency due to weak light-matter interactions in graphene when the light is normally incident to this atomic-layer-thick material.

Serval methods have been proposed and demonstrated to overcome the limitation of weak light-matter interactions, such as graphene plasmonic devices [10–13], fiber-integrated graphene devices [14], and waveguide-integrated graphene devices [15–17]. Comparing to the graphene plasmonic devices and fiber-integrated graphene devices, the waveguide-integrated graphene devices are developed based on complementary metal-oxide-semiconductor (CMOS) compatible photonic integrated circuits (PICs), which have advantages of high-density integration, high-quality devices, and low-cost fabrication processes [18]. After integrating graphene on top of PICs, the propagating light in the waveguide can significantly interact with the graphene layer via the evanescence-field coupling. For example, recent studies show that the optical absorption in graphene-on-silicon PICs can increase to nearly 100% which is much higher than ~2.3% optical absorption of normal incident light [19]. As a result, waveguide-integrated graphene devices have received great attention to explore optoelectronic properties of graphene.

On the other hand, waveguide-integrated graphene devices are expected to break the bottle neck of traditional silicon-based PICs. Silicon photonics has been widely studied for the applications in optical interconnects [20], optical communications [21], and nonlinear optics [22] in

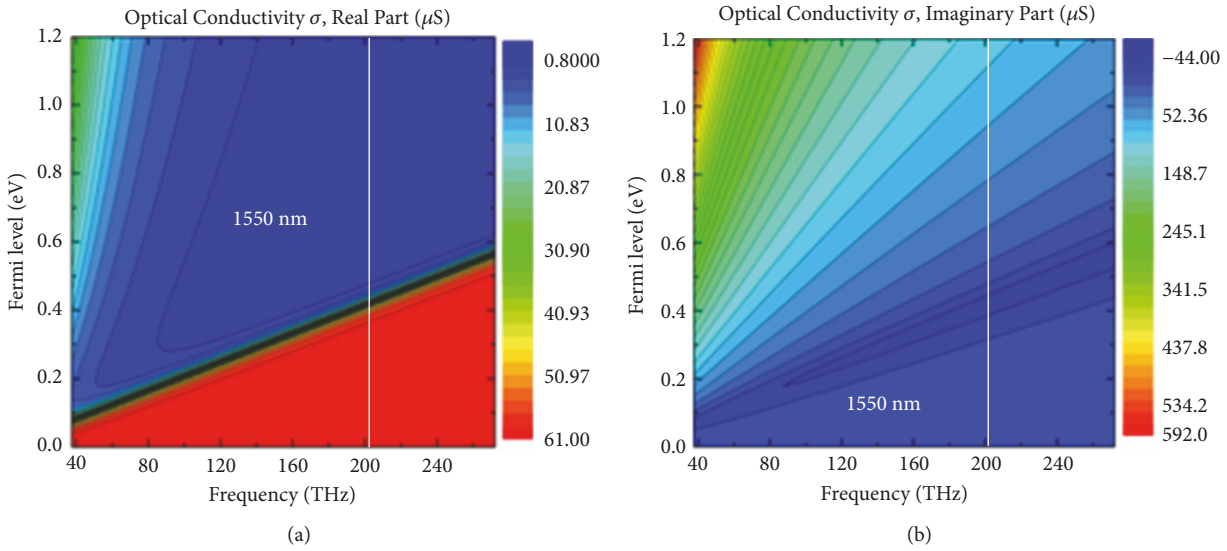

Figure 1: Calculated optical conductivity of graphene as a function of Fermi level. (a) The real part of the optical conductivity. (b) The imaginary part of the optical conductivity.

the past decades. However, these applications are facing many challenges. Taking silicon modulators, for example, due to the limitation of carrier plasma dispersion effect in silicon, the theoretical upper limitation of the modulation bandwidth using p-n or p-i-n diodes may be ~50 GHz [23], which cannot satisfy the growing demand in the modern information society. Graphene provides a promising solution to this issue. The carrier mobility of pristine graphene can be as high as 200,000 cm^2/Vs which results in the maximum modulation bandwidth of 500 GHz [9]. Besides, in waveguide configurations, light-graphene interactions are enhanced through evanescent field coupling, resulting in larger saturation energy and ultrafast optical pulses with higher energy [24, 25]. Therefore, the study of waveguide-integrated graphene devices paves a new way to develop on-chip optoelectronic applications.

In this paper, we introduce basic principles and recent research advances of waveguide-integrated graphene optoelectronic devices on various platforms, especially waveguide-integrated graphene photodetectors and modulators. Optical properties of graphene-covered optical waveguides are first introduced in Section 2. In Section 3, we discuss waveguide-integrated graphene modulators. The studies of electro-absorptive modulators as well as electro-refractive modulators are reviewed in this section. In Section 4, we review research progress on waveguide-integrated graphene photodetectors. Different detection mechanisms and waveguide structures, which are developed for improving the responsivity of graphene photodetectors, are introduced in this part. Finally, summary and prospects of the waveguide-integrated graphene optoelectronics are discussed in Section 5.

2. Graphene-Covered Optical Waveguides

Optical properties of graphene can be described by optical conductivity σ, calculated from Kubo formalism [26]. The optical conductivity σ includes contributions from interband transition and intraband transition in graphene which can be expressed by

$$\sigma = -\frac{2ie^2(\Omega + 2i\Gamma)}{h}\left[\frac{1}{(\Omega + 2i\Gamma)^2} \cdot \int_{\Delta}^{\infty} \frac{\omega^2 + \Delta^2}{\omega}\left(\frac{\delta n_F(\omega)}{\delta\omega} - \frac{\delta n_F(-\omega)}{\delta\omega}\right)d\omega - \int_{\Delta}^{\infty} \frac{\omega^2 + \Delta^2}{\omega}\left(\frac{n_F(-\omega) - n_F(\omega)}{(\Omega + 2i\Gamma)^2 - 4\omega^2}\right)d\omega\right], \quad (1)$$

where Ω is optical frequency, $n_F(\omega)$ is the Fermi distribution function, $\Gamma(\omega)$ is the scattering rate, ω is the energy of the relativistic Landau levels, and Δ is the exciton gap of Landau level energies. The calculated graphene's optical conductivity σ with respect to Fermi level and frequency is shown in Figure 1. For a given wavelength, for example, 1550 nm as indicated in Figure 1, when the Fermi level is less than half of the photon energy (~0.4 eV), the real part of the optical conductivity is almost a universal value (~61 μS) which is governed by the interband transition. When the Fermi level is larger than half of the photon energy, the real part of the optical conductivity drops significantly since interband transition is blocked due to Pauli blocking effect.

By assuming a finite thickness to the graphene layer, the effective relative permittivity ε_{eff} of graphene can be calculated as follows [1]:

$$\varepsilon_{\text{eff}} = 1 + i\frac{\sigma}{\omega\varepsilon_0 d}, \quad (2)$$

where d is the thickness of graphene layer. By using the calculated relative permittivity ε_{eff}, the effective complex refractive index (RI) of a graphene-covered waveguide can be numerically simulated such that we can design waveguide-integrated graphene devices before fabrication.

In the past few years, graphene-covered optical waveguides were theoretically and experimentally studied in the telecommunication band. Li et al. [19] characterized the optical absorption coefficient of graphene-on-silicon transverse electric (TE) mode waveguides to be 0.2 dB/μm which agreed well with simulation results. Besides, Cheng et al. studied the polarization-dependent optical absorption of graphene-on-silicon waveguides [27]. Due to the different intensity distributions, graphene has distinct optical absorptions to TE and transverse magnetic (TM) modes propagating light. In this study, graphene introduces 7.7 dB higher losses for TM mode in a 150-μm-long waveguide.

To further enhance the interaction between propagating light in the waveguide and graphene, researchers proposed and demonstrated various waveguide-integrated graphene devices. For example, Wang et al. [28] designed the structure of graphene-on-silicon nitride microring resonator by tailoring the length of graphene integrated on the microring resonator to obtain the maximum optical absorption, as shown in the schematic image of Figure 2(a). The variation in quality (Q) factor of the microring resonator as a function of the graphene length was measured experimentally, which agreed well with the theoretical calculation, as shown in Figures 2(b)–2(f). The fundamental characterizations of graphene-on-silicon nitride microring resonators in this paper were useful for developing high-performance graphene optoelectronic devices. For example, based on this graphene-on-silicon nitride microring resonator structure, a waveguide-integrated graphene photodetector was demonstrated [29]. Besides microring resonators, people have proposed and demonstrated the use of other resonant cavities, such as silicon photonic crystal nanocavities [30], in enhancing the graphene absorption.

3. Waveguide-Integrated Graphene Modulators

Waveguide-integrated modulators with high speed, small footprint, and large spectral bandwidth are key components for applications of optical interconnects and optical communications [31], which can be classified as electro-refractive modulators or electro-absorptive modulators. In the electro-refractive modulators, an applied electrical field changes the real part of the effective RI of optical mode in the waveguide such that the phase of the propagating light is modulated. In the electro-absorptive modulators, an applied electrical field changes the imaginary part of the effective RI of optical mode in the waveguide, resulting in variations in optical loss. For traditional waveguide-integrated modulators based on silicon photonic technology, the most common method is based on the plasmon dispersion effect, in which some carriers are injected to silicon waveguide to alter the real and imaginary parts of the RI of waveguide mode [32]. The intrinsic modulation bandwidth limit may be up to 50 GHz. Besides, due to the relatively weak light-matter interaction, usually mm-long interaction length is needed to achieve full transition between the maximum and minimum optical transmission [33]. On the other hand, graphene has relatively low carrier density, which makes it possible to tune its permittivity by applying an external electrical field. When graphene is integrated on a waveguide, the changes of the complex effective RI of the waveguide mode can be achieved through electrically tuning the Fermi level of graphene, enabling electro-refractive modulators or electro-absorptive modulators. What is more, by optimizing the waveguide structures, an extremely strong light-graphene interaction may be obtained, leading to a significant reduction in device footprint. In this section, we summarize the recent progress on waveguide-integrated graphene modulators.

The first waveguide-integrated graphene modulator was demonstrated by Liu et al. [34] in 2011, in which electro-absorptive modulation was achieved by tuning the Fermi level of graphene through electro-gating from the lightly doped SOI waveguide. The device had a bandwidth of 1.2 GHz. The authors subsequently demonstrated the structure of dual-layer graphene sandwiching by a thin layer for the waveguide-integrated modulator in 2012 [35], in which electrons and holes were injected into the graphene layers to form a p-oxide-n junction. The schematic of the cross section of dual-layer graphene modulator was shown in Figure 3(a). At zero drive voltage, the Fermi levels of both graphene layers were close to Dirac point such that the interband transition led to large optical absorption, as shown in Figure 3(b). At high drive voltage, the two layers of graphene were symmetrically doped with electrons and holes, respectively, shifting the Fermi levels beyond the half of the photon energy $|\hbar\omega/2|$, resulting in optical transparence of graphene. A 3-dB bandwidth of 1 GHz was experimentally achieved in this device. The configuration of dual-layer graphene has also been further explored with interferometric and resonant waveguide structures. Youngblood et al. [36] applied the dual-layer graphene structure in an unbalanced Mach-Zehnder interferometer (MZI) to achieve simultaneous optical modulation and detection, as shown in Figure 3(c). The modulation depth of 64% was achieved in the 90-μm-long waveguide. Also, Phare et al. [37] demonstrated the dual-layer graphene electro-absorptive modulator with a similar configuration in a low-loss silicon nitride microring resonator. The overall transmissions of the resonant wavelengths were modulated by the gate voltage with the bandwidth of 30 GHz.

To achieve efficient graphene electro-absorptive modulators, some novel waveguide structures have been theoretically proposed to enhance light-matter interactions. Lu and Zhao [39] proposed a modulator based on graphene horizontally sandwiched in dielectric waveguides, in which the relative permittivity of graphene can be tuned to enhance the absorption modes. A 3-dB modulation depth can be achieved within a 800-nm-long waveguide. Furthermore, Abdollahi Shiramin and Van Thourhout [40] theoretically investigated a similar structure of double-layer graphene sandwiching by a thin dielectric layer on the silicon nitride waveguide. The optimized bandwidth was calculated to be 2.5 GHz. Besides, photonic crystal (PC) nanocavity and microring resonators can also provide enhanced light-matter interactions. Gan et al. [38] used the silicon air-slot nanocavity to enhance the overlap between graphene and cavity resonance modes, due to the strong confinement of optical modes in the central air-gap, as shown in Figure 3(d). The reflectivity and Q

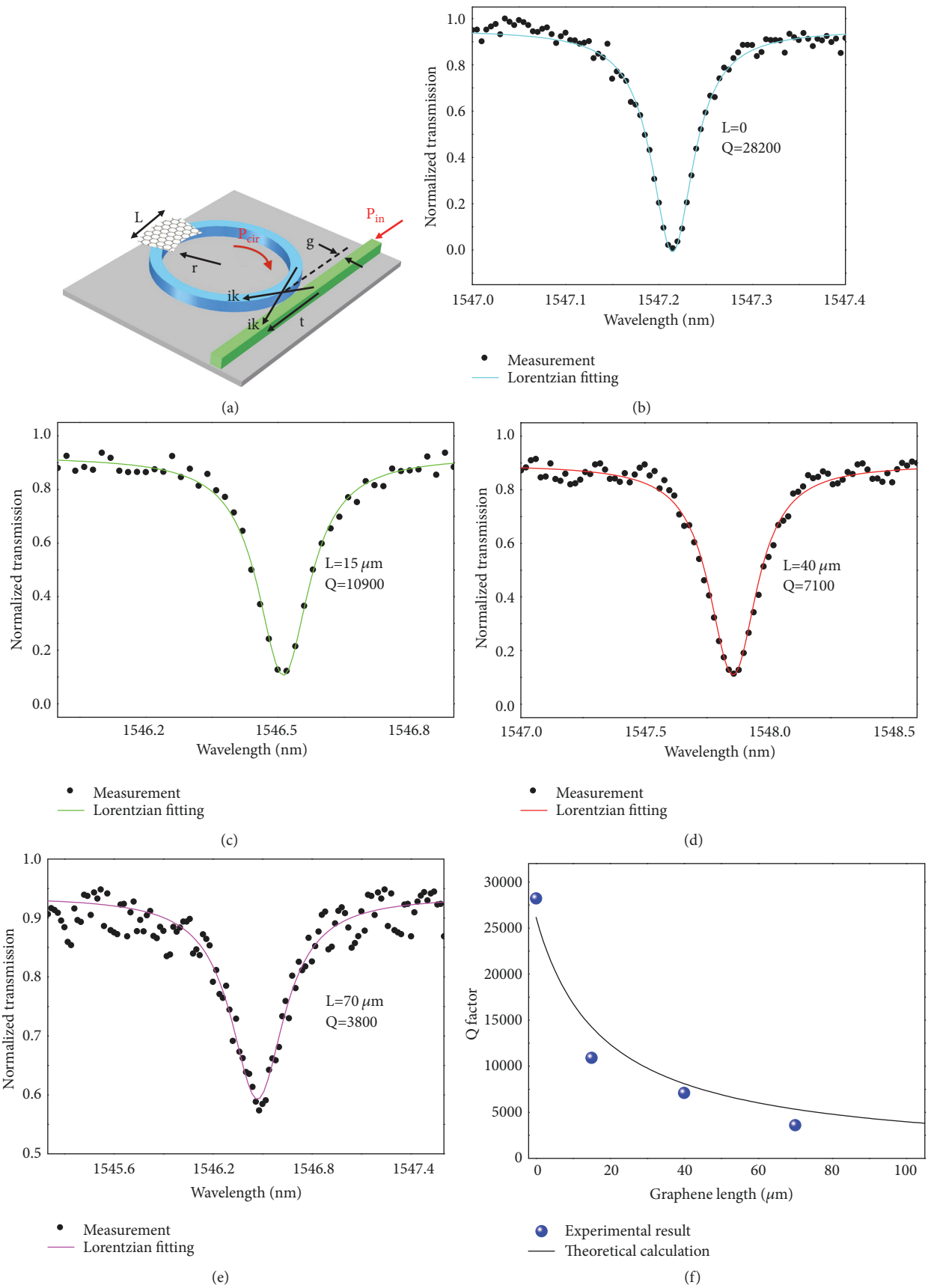

FIGURE 2: Graphene-on-silicon nitride microring resonators. (a) Schematic of the graphene-on-silicon nitride microring resonator. (b)–(e) Experimental measurements of resonance spectra of the graphene-on-silicon nitride microring resonators with graphene lengths of 0 μm, 15 μm, 40 μm, and 70 μm. (f) Experimental and theoretical results of the Q factor as a function of graphene length. Figure 2 is reprinted from [28]. Copyright © 2015 IEEE.

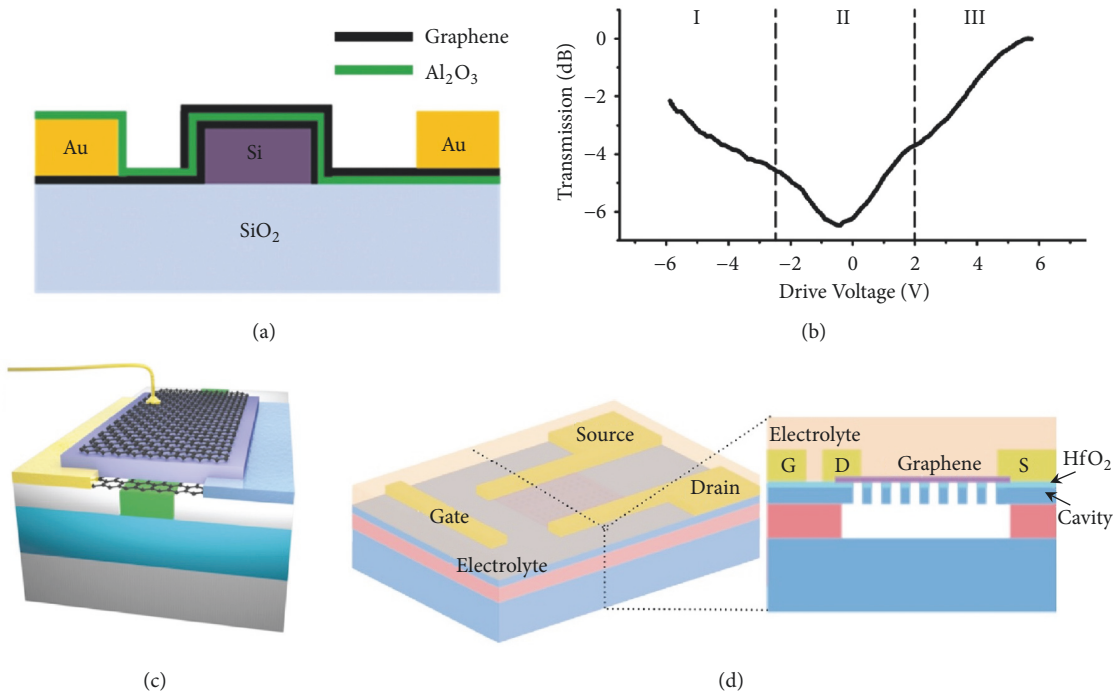

Figure 3: Schematics of waveguide-integrated graphene modulators. (a) Schematic of the dual-layer graphene modulator. (b) Graphene absorption as a function of driving voltage for the dual-layer graphene modulator. (c) Schematic of the multifunctional graphene modulator and photodetector. (d) Schematic of the graphene modulator integrated with air-suspended photonic crystal nanocavity. (a) and (b) are reprinted with permission from [35]. Copyright © 2012 American Chemical Society. (c) is reprinted with permission from [36]. Copyright © 2014 American Chemical Society. (d) is reprinted with permission from [38]. Copyright © 2013 American Chemical Society.

factor of the cavity were modulated by the gated graphene, achieving 10 dB modulation depth under the 1.5 V gate voltage. Moreover, Qiu et al. [41] demonstrated a graphene electro-absorptive modulator based on an all-pass microring resonator structure. The Q factor and resonant wavelength of the silicon microring resonator were strongly modulated by tuning the Fermi level of graphene.

When the Fermi level of graphene is tuned beyond half of the photon energy of incident light, the interband transition is blocked, which can be used for achieving electro-refractive modulation, since the insertion loss becomes constant but phase variation changes obviously when tuning the Fermi level of graphene. Xu et al. [42] designed the graphene-oxide-silicon waveguide structure with an MZI to achieve electro-refractive modulation from constructive or destructive interferences in the device. Later, Phatak et al. [43] studied the electro-refractive modulators based on the graphene-on-silicon slot waveguide. The slot vertical waveguide consists of two rib waveguides vertically sandwiching by a thin layer of low index region which allows confining and guiding a high intensity of TE mode light in the slot region due to the discontinuity of the electric field at the high-RI contrast interface. Thus, graphene has a much stronger interaction with the propagating light after being integrated on the surface of the slot waveguide, comparing to that in graphene-on-silicon channel or rib waveguide. The graphene-on-silicon slot waveguide was applied in MZIs and microring resonators to achieve efficient modulation with compact footprints. Moreover, Pan et al. [44] designed the electro-refractive modulator based on one-dimensional photonic crystal nanobeam cavity coupled to a bus waveguide with a graphene sheet on top. By electrically tuning the Fermi level of graphene, the Q factor and resonant wavelength were modulated, achieving the modulation depth as large as 12.5 dB in the telecommunication band.

Researchers have also experimentally exploited graphene electro-refractive modulators. Mohsin et al. [45] experimentally demonstrated the electro-refractive modulator based on the structure of graphene-on-silicon add-drop microring resonator. A voltage length product for a phase shift of π, $V\pi L = 2.7$ Vmm was extracted. Gan et al. [16] demonstrated a highly efficient thermal-optic silicon microring modulator assisted by graphene. The effective RI of the silicon microring resonator was modulated through heating effect, leading to large resonant wavelength modulation of 2.7 nm and modulation depth up to 7 dB. Recently, Sorianello et al. [46] experimentally demonstrated a waveguide-integrated graphene electro-refractive modulator based on the MZI structure, which had a bandwidth of 10 Gb/s.

4. Waveguide-Integrated Graphene Photodetectors

With the features of zero bandgap and high electron mobility, graphene photodetectors are promising for broadband photodetection with ultrahigh bandwidth, which is only limited

by the resistor-capacitor (RC) time constant of electrodes. Integration of graphene on an optical waveguide can dramatically increase the optical absorption through the in-plane light coupling, the detection efficiency of the graphene photodetector therefore can be increased. In this section, different mechanisms of photodetection in graphene are first introduced. Then, recent advances in waveguide-integrated graphene photodetectors are reviewed.

In the early works, graphene photodetectors were mainly developed based on field effect transistor (FET) structures [9], in which three major mechanisms, namely, photovoltaic effect, photo-thermoelectric effect, and bolometric effect [47], were studied by transport measurements under different bias conditions. For the photovoltaic effect, photocurrents are generated through accelerating photogenerated electron-hole pairs to respective electrodes by a built-in electrical field at the junction where doping levels of graphene are different at two sides [47]. The device often works in the bias-free condition. The built-in field can be formed at the graphene junction with different Fermi levels at two sides or at a graphene-metal junction. In the case of photo-thermoelectric effect, the photocurrent is generated at the interface of graphene with different doping levels, which have different thermoelectric powers, such as the single/bilayer graphene junction. Upon light illumination, the photocurrent is proportional to the difference in thermoelectric power of the two sides and photogenerated electrons diffuse from areas with lower density of states to areas with higher density of states, according to the second law of thermodynamics [48]. In the case of bolometric effect, the light illumination can heat the active region and alter the transport conductance of the device, such as the photoresponse in a graphene/metal junction [47]. The bolometric effect can operate on the homogeneous graphene. The change of conductance is contributed to the variation in carrier mobility of graphene by temperature change and therefore conductance change induced by incident light.

By integrating graphene on SOI waveguides, graphene photodetectors with high responsivity and high bandwidth were demonstrated in telecommunication bands and mid-infrared spectral region for the first time in 2013. Gan et al. [15] fabricated the lateral graphene-metal junction overlapped with the waveguide mode to form the built-in electrical field to separate photogenerated electron-hole pairs. The device had a responsivity of 0.1 A/W with bandwidth of 20 GHz. Pospischil et al. [49] used the graphene-metal junction between the electrode on top of the SOI waveguide and lateral graphene to create the built-in electrical field to separate photocarriers. This device was operated in all telecommunication bands with 3-dB bandwidth of 18 GHz. Wang et al. [50] integrated graphene-on-silicon suspended membrane waveguide (SMW). The silicon SWM, which is proposed and demonstrated by Cheng et al. [51], can eliminate the absorption of buried oxide in the mid-infrared spectral range and take full advantage of the silicon transparent window of 1–8 μm. So, the demonstrated graphene-on-silicon photodetectors can be operated in the mid-infrared spectral region. Moreover, the graphene/silicon heterostructure was employed in the work which reduced the dark current and achieving a high ON/OFF current ratio in a broadband spectral range. The authors demonstrated a responsivity as high as 0.13 A/W at the wavelength of 2.75 μm, operating with a bias of only 1.5 V at room temperature. Besides the above mechanically exfoliating graphene-based photodetectors, researchers have tried to use CVD-growth graphene to develop high-performance waveguide-integrated graphene photodetectors. For example, Schall et al. [52] integrated graphene on the planarized silicon waveguide with a lateral asymmetrical electrode setting. The device had a 3-dB bandwidth of 41 GHz. Goykhman et al. [53] used the graphene/metal contacting with the silicon waveguide to form a Schottky diode and explored the internal photon emission process, as shown in Figure 4(a). The maximum responsivity of 0.37 A/W and avalanche photo-gain of ~2 were achieved.

Besides channel and rib waveguides, researchers have exploited numerous novel waveguide structures to develop high-performance graphene photodetectors. Wang et al. [54] demonstrated the high-responsivity graphene photodetector integrated on the silicon slot waveguide, as shown in the schematic of Figure 4(b). According to the simulation, among the four types of waveguides, namely, graphene-on-silicon TE/TM mode channel waveguides and graphene-on-silicon TE/TM slot waveguides, the graphene-on-TE mode waveguide showed the maximum optical absorption after optimization, as shown in Figure 4(b). Similar to the discussions in Section 3, the enhanced light-graphene interaction and poor confinement of optical mode in the TE mode slot waveguide contributed to the larger optical absorption and therefore enhanced responsivity of the photodetector, comparing to the graphene-on-silicon channel waveguides. In experiment, graphene was patterned to only 20 μm long on top of the slot waveguide with the nanoslot width of 80 nm. The maximum responsivity of 0.273 A/W was achieved in the telecommunication band. Later, Schuler et al. [55] took use of the two rib waveguides of the slot waveguide as dual back gates, creating a p-n junction at the optical absorption region. The photodetector showed the maximum responsivity of 76 mA/W with the 3-dB cutoff frequency of 65 GHz.

Apart from graphene photodetectors integrated on the SOI platform, researchers have developed graphene photodetectors based on other integration platforms. For example, silicon nitride is a large bandgap (~5 eV) deposited material that is compatible with CMOS fabrication technology. Wang et al. [56] demonstrated the broadband graphene photodetector integrated on the silicon nitride waveguide. The two electrodes were set asymmetrically along the waveguide. By identifying the polarity of the photocurrent, different detection mechanisms, such as bolometric effect and photo-thermoelectric effect, can be identified. Besides, the authors demonstrated the graphene photodetector based on graphene-on-silicon nitride microring resonator [29]. The scanning electron microscopy (SEM) image of the fabricated device is shown in Figure 4(d). The authors demonstrated the maximum responsivity of 1.31 mA/W at the wavelength of 1.55 μm. Besides silicon nitride, Cheng et al. [57] demonstrated the graphene photodetector integrated on the silicon-on-sapphire (SOS) waveguide operating at the wavelength of 2.75 μm in room temperature. The SOS waveguide is

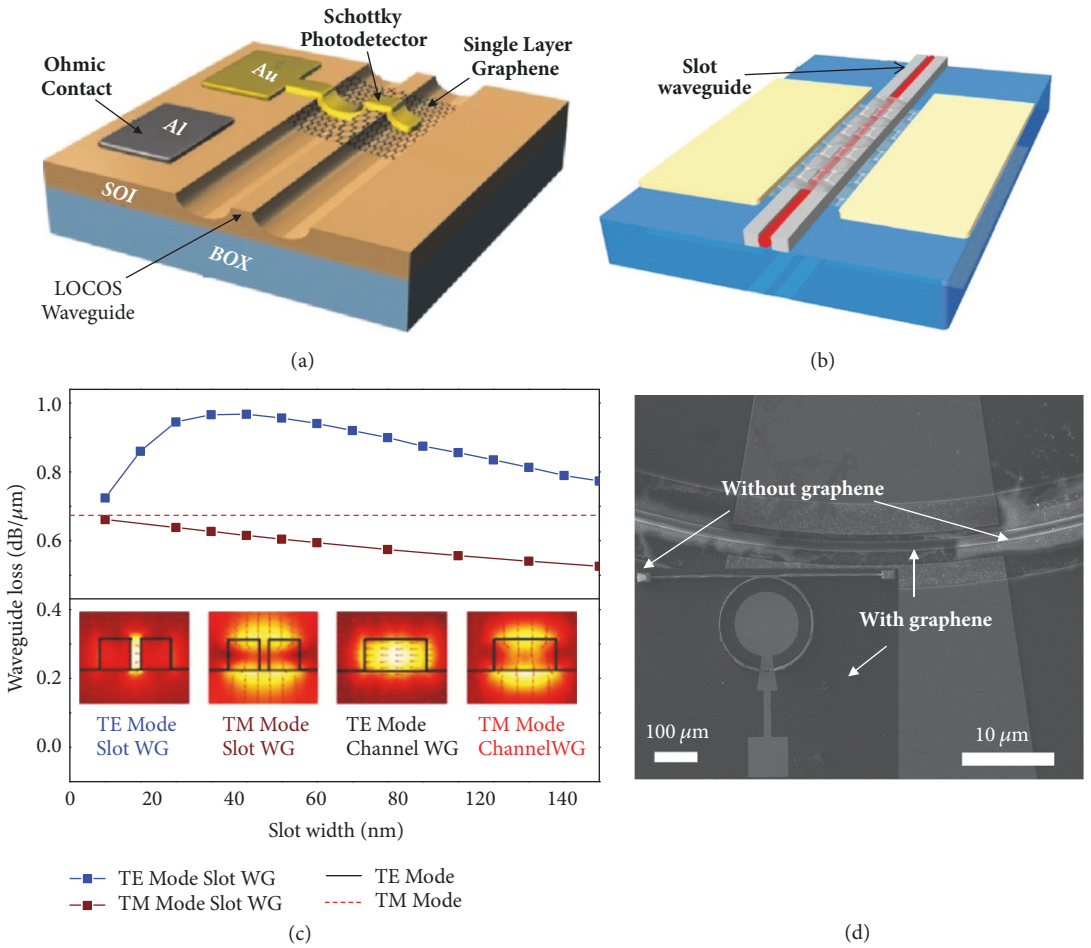

FIGURE 4: Waveguide-integrated graphene photodetectors. (a) Schematic of the graphene Schottky diode integrated on the SOI waveguide. (b) Schematic of the graphene-on-silicon slot waveguide photodetector. (c) Simulation results of the graphene-on-waveguide absorption coefficients. (d) SEM image of the graphene-on-silicon nitride microring resonator photodetector. (a) is reprinted with permission from [53]. Copyright © 2016 American Chemical Society. (b)-(c) are reprinted with permission from Ref. [54]. Copyright © 2016 Royal Society of Chemistry. (d) is reprinted from [29]. Copyright © 2016 Optical Society of America.

transparent in the spectral region from 1.0 to 5.5 μm, due to the transparency of the sapphire substrate. With metal contacts fabricated on graphene and silicon waveguide, the graphene/silicon heterostructure was adopted to form a built-in electrical field to separate generated electron/hole pairs in this work.

5. Summary and Future Prospective

In conclusion, with the unique optical and electrical properties, graphene is expected to improve the performance of conventional PICs and bring new applications. In this paper, we present recent progress in the waveguide-integrated graphene optoelectronics, specifically waveguide-integrated graphene modulators and photodetectors. Although the past few years have seen a lot of advances in this field, great efforts still need to be made for improvement. For example, the ultra-high mobility of graphene indicates up to 500 GHz working bandwidth of graphene optoelectronic devices, but the current demonstrated waveguide-integrated graphene photodetectors and modulators only have a few tens of GHz working bandwidth, maybe limited by the process of manual transfer of CVD-growth graphene onto the PICs, which could cause contamination and breakage of graphene. Besides, the manual transfer process is convenient for lab research but still not suitable for mass production in industry. With the rapid development in graphene synthesis technologies, direct deposition of graphene on various types of substrates, especially silicon, will further boost advances in high-speed graphene optoelectronics and silicon photonics. On the other hand, there are other two-dimensional materials developed very recently, with very different optical and electrical properties from graphene, such as layered transition metal dichalcogenides [58], boron nitride (h-BN) nanosheets [59], and black phosphorus [60]. Hopefully, integration such two-dimensional materials with PICs will lead to other breakthroughs in large-scale applications.

Conflicts of Interest

The authors declare that they have no conflicts of interest.

Acknowledgments

This work is jointly supported by the National Science Foundation of China (no. 61775149) and Natural Science Foundation of SZU (no. 85302-000170).

References

[1] Y. Zhang, T.-T. Tang, C. Girit et al., "Direct observation of a widely tunable bandgap in bilayer graphene," *Nature*, vol. 459, no. 7248, pp. 820–823, 2009.

[2] F. Bonaccorso, Z. Sun, T. Hasan, and A. C. Ferrari, "Graphene photonics and optoelectronics," *Nature Photonics*, vol. 4, no. 9, pp. 611–622, 2010.

[3] A. H. Castro Neto, F. Guinea, N. M. R. Peres, K. S. Novoselov, and A. K. Geim, "The electronic properties of graphene," *Reviews of Modern Physics*, vol. 81, no. 1, pp. 109–162, 2009.

[4] Q. Bao, "Atomic layer graphene as saturable absorber for ultrafast pulsed lasers," *Advanced Functional Materials*, vol. 639798, p. 24, 2009.

[5] Z. Sun, T. Hasan, F. Torrisi et al., "Graphene mode-locked ultrafast laser," *ACS Nano*, vol. 4, no. 2, pp. 803–810, 2010.

[6] Q. Bao, H. Zhang, Z. Ni et al., "Monolayer graphene as a saturable absorber in a mode-locked laser," *Nano Research*, vol. 4, no. 3, pp. 297–307, 2011.

[7] Z. Li, C. Cheng, N. Dong et al., "Q-switching of waveguide lasers based on graphene/WS2 van der Waals heterostructure," *Photonics Research*, vol. 5, no. 5, pp. 406–410, 2017.

[8] A. G. Okhrimchuk and P. A. Obraztsov, "11-GHz waveguide Nd: YAG laser CW mode-locked with single-layer graphene," *Scientific Reports*, vol. 5, Article ID 11172, 2015.

[9] F. Xia, T. Mueller, Y.-M. Lin, A. Valdes-Garcia, and P. Avouris, "Ultrafast graphene photodetector," *Nature Nanotechnology*, vol. 4, no. 12, pp. 839–843, 2009.

[10] T. J. Echtermeyer, L. Britnell, P. K. Jasnos et al., "Strong plasmonic enhancement of photovoltage in graphene," *Nature Communications*, vol. 2, no. 1, article no. 458, 2011.

[11] F. H. L. Koppens, D. E. Chang, and F. J. García de Abajo, "Graphene plasmonics: a platform for strong light–matter interactions," *Nano Letters*, vol. 11, no. 8, pp. 3370–3377, 2011.

[12] A. N. Grigorenko, M. Polini, and K. S. Novoselov, "Graphene plasmonics," *Nature Photonics*, vol. 6, no. 11, pp. 749–758, 2012.

[13] T.-H. Xiao, Z. Cheng, and K. Goda, "Graphene-on-silicon hybrid plasmonic-photonic integrated circuits," *Nanotechnology*, vol. 28, no. 24, Article ID 245201, 2017.

[14] Q. Bao, H. Zhang, B. Wang et al., "Broadband graphene polarizer," *Nature Photonics*, vol. 5, no. 7, pp. 411–415, 2011.

[15] X. Gan, R.-J. Shiue, Y. Gao et al., "Chip-integrated ultrafast graphene photodetector with high responsivity," *Nature Photonics*, vol. 7, no. 11, pp. 883–887, 2013.

[16] S. Gan, C. Cheng, Y. Zhan et al., "A highly efficient thermo-optic microring modulator assisted by graphene," *Nanoscale*, vol. 7, no. 47, pp. 20249–20255, 2015.

[17] Q. Bao, K. P. Loh, G. Eda, and M. Chhowalla, "Graphene photonics, plasmonics, and broadband optoelectronic devices," *ACS Nano*, vol. 6, pp. 3677–3694, 2012.

[18] S. J. Koester and M. Li, "Waveguide-coupled graphene optoelectronics," *IEEE Journal of Selected Topics in Quantum Electronics*, vol. 20, no. 1, 2014.

[19] H. Li, Y. Anugrah, S. J. Koester, and M. Li, "Optical absorption in graphene integrated on silicon waveguides," *Applied Physics Letters*, vol. 101, no. 11, p. 111110, 2012.

[20] M. J. R. Heck, H.-W. Chen, A. W. Fang et al., "Hybrid silicon photonics for optical interconnects," *IEEE Journal of Selected Topics in Quantum Electronics*, vol. 17, no. 2, pp. 333–346, 2011.

[21] K. Van Acoleyen, H. Rogier, and R. Baets, "Two-dimensional optical phased array antenna on silicon-on-insulator," *Optics Express*, vol. 18, no. 13, pp. 13655–13660, 2010.

[22] L. Xu, N. Ophir, M. Menard et al., "Simultaneous wavelength conversion of ASK and DPSK signals based on four-wave-mixing in dispersion engineered silicon waveguides," *Optics Express*, vol. 19, no. 13, pp. 12172–12179, 2011.

[23] X. Tu, T.-Y. Liow, J. Song et al., "50-Gb/s silicon optical modulator with traveling-wave electrodes," *Optics Express*, vol. 21, no. 10, pp. 12776–12782, 2013.

[24] Y. Tan, C. Cheng, S. Akhmadaliev, S. Zhou, and F. Chen, "Nd:YAG waveguide laser Q-switched by evanescent-field interaction with graphene," *Optics Express*, vol. 22, no. 8, pp. 9101–9106, 2014.

[25] H. Liu, C. Cheng, C. Romero, J. R. V. De Aldana, and F. Chen, "Graphene-based Y-branch laser in femtosecond laser written Nd:YAG waveguides," *Optics Express*, vol. 23, no. 8, pp. 9730–9735, 2015.

[26] V. P. Gusynin, S. G. Sharapov, and J. P. Carbotte, "Magneto-optical conductivity in graphene," *Journal of Physics: Condensed Matter*, vol. 19, no. 2, Article ID 026222, 2007.

[27] Z. Cheng, H. K. Tsang, X. Wang, X. Chen, K. Xu, and J. Xu, "Polarization dependent loss of graphene-on-silicon waveguides," in *Proceedings of the 2013 IEEE Photonics Conference (IPC)*, pp. 460-461, Bellevue, WA, USA, September 2013.

[28] J. Wang, Z. Cheng, C. Shu, and H. K. Tsang, "Optical Absorption in Graphene-on-Silicon Nitride Microring Resonators," *IEEE Photonics Technology Letters*, vol. 27, no. 16, pp. 1765–1767, 2015.

[29] J. Wang, Z. Cheng, B. Zhu, C. Shu, and H. K. Tsang, "Photoresponse of graphene-on-silicon nitride microring resonator," in *Proceedings of the 2016 Conference on Lasers and Electro-Optics, CLEO 2016*, usa, June 2016.

[30] X. Gan, K. F. Mak, Y. Gao et al., "Strong enhancement of light-matter interaction in graphene coupled to a photonic crystal nanocavity," *Nano Letters*, vol. 12, no. 11, pp. 5626–5631, 2012.

[31] G. T. Reed, G. Mashanovich, F. Y. Gardes, and D. J. Thomson, "Silicon optical modulators," *Nature Photonics*, vol. 4, no. 8, pp. 518–526, 2010.

[32] R. A. Soref and B. R. Bennett, "Electrooptical effects in silicon," *IEEE Journal of Quantum Electronics*, vol. 23, no. 1, pp. 123–129, 1987.

[33] L. Liao, D. Samara-Rubio, M. Morse et al., "High speed silicon Mach-Zehnder modulator," *Optics Express*, vol. 13, no. 8, pp. 3129–3135, 2005.

[34] M. Liu, X. Yin, E. Ulin-Avila et al., "A graphene-based broadband optical modulator," *Nature*, vol. 474, no. 7349, pp. 64–67, 2011.

[35] M. Liu, X. B. Yin, and X. Zhang, "Double-layer graphene optical modulator," *Nano Letters*, vol. 12, no. 3, pp. 1482–1485, 2012.

[36] N. Youngblood, Y. Anugrah, R. Ma, S. J. Koester, and M. Li, "Multifunctional graphene optical modulator and photodetector integrated on silicon waveguides," *Nano Letters*, vol. 14, no. 5, pp. 2741–2746, 2014.

[37] C. T. Phare, Y.-H. Daniel Lee, J. Cardenas, and M. Lipson, "Graphene electro-optic modulator with 30 GHz bandwidth," *Nature Photonics*, vol. 9, no. 8, pp. 511–514, 2015.

[38] X. Gan, R.-J. Shiue, Y. Gao et al., "High-contrast electrooptic modulation of a photonic crystal nanocavity by electrical gating of graphene," *Nano Letters*, vol. 13, no. 2, pp. 691–696, 2013.

[39] Z. Lu and W. Zhao, "Nanoscale electro-optic modulators based on graphene-slot waveguides," *Journal of the Optical Society of America B: Optical Physics*, vol. 29, no. 6, pp. 1490–1496, 2012.

[40] L. Abdollahi Shiramin and D. Van Thourhout, "Graphene Modulators and Switches Integrated on Silicon and Silicon Nitride Waveguide," *IEEE Journal of Selected Topics in Quantum Electronics*, vol. 23, no. 1, 2017.

[41] C. Qiu, W. Gao, R. Vajtai, P. M. Ajayan, J. Kono, and Q. Xu, "Efficient modulation of 1.55 μm radiation with gated graphene on a silicon microring resonator," *Nano Letters*, vol. 14, no. 12, pp. 6811–6815, 2014.

[42] C. Xu, Y. Jin, L. Yang, J. Yang, and X. Jiang, "Characteristics of electro-refractive modulating based on Graphene-Oxide-Silicon waveguide," *Optics Express*, vol. 20, no. 20, pp. 22398–22405, 2012.

[43] A. Phatak, Z. Cheng, C. Qin, and K. Goda, "Design of electro-optic modulators based on graphene-on-silicon slot waveguides," *Optics Expresss*, vol. 41, no. 11, pp. 2501–2504, 2016.

[44] T. Pan, C. Qiu, J. Wu et al., "Analysis of an electro-optic modulator based on a graphene-silicon hybrid 1D photonic crystal nanobeam cavity," *Optics Express*, vol. 23, no. 18, pp. 23357–23364, 2015.

[45] M. Mohsin, D. Schall, M. Otto, B. Chmielak, S. Suckow, and D. Neumaier, "Towards the Predicted High Performance of Waveguide Integrated Electro-Refractive Phase Modulators Based on Graphene," *IEEE Photonics Journal*, vol. 9, no. 1, 2017.

[46] V. Sorianello, M. Midrio, G. Contestabile et al., "Graphene-silicon phase modulators with gigahertz bandwidth," *Nature Photonics*, vol. 12, no. 1, pp. 40–44, 2018.

[47] M. Freitag, T. Low, F. Xia, and P. Avouris, "Photoconductivity of biased graphene," *Nature Photonics*, vol. 7, no. 1, pp. 53–59, 2013.

[48] X. Xu, N. M. Gabor, J. S. Alden, A. M. Van Der Zande, and P. L. McEuen, "Photo-thermoelectric effect at a graphene interface junction," *Nano Letters*, vol. 10, no. 2, pp. 562–566, 2010.

[49] A. Pospischil, M. Humer, M. M. Furchi et al., "CMOS-compatible graphene photodetector covering all optical communication bands," *Nature Photonics*, vol. 7, no. 11, pp. 892–896, 2013.

[50] X. Wang, Z. Cheng, K. Xu, H. K. Tsang, and J.-B. Xu, "High-responsivity graphene/silicon-heterostructure waveguide photodetectors," *Nature Photonics*, vol. 7, no. 11, pp. 888–891, 2013.

[51] Z. Cheng, X. Chen, C. Y. Wong, K. Xu, and H. K. Tsang, "Mid-infrared Suspended Membrane Waveguide and Ring Resonator on Silicon-on-Insulator," *IEEE Photonics Journal*, vol. 4, no. 5, pp. 1510–1519, 2012.

[52] D. Schall, D. Neumaier, M. Mohsin et al., "50 GBit/s Photodetectors Based on Wafer-Scale Graphene for Integrated Silicon Photonic Communication Systems," *ACS Photonics*, vol. 1, no. 9, pp. 781–784, 2014.

[53] I. Goykhman, U. Sassi, B. Desiatov et al., "On-Chip Integrated, Silicon-Graphene Plasmonic Schottky Photodetector with High Responsivity and Avalanche Photogain," *Nano Letters*, vol. 16, no. 5, pp. 3005–3013, 2016.

[54] J. Wang, Z. Cheng, Z. Chen et al., "High-responsivity graphene-on-silicon slot waveguide photodetectors," *Nanoscale*, vol. 8, no. 27, pp. 13206–13211, 2016.

[55] S. Schuler, D. Schall, D. Neumaier et al., "Controlled Generation of a p-n Junction in a Waveguide Integrated Graphene Photodetector," *Nano Letters*, vol. 16, no. 11, pp. 7107–7112, 2016.

[56] J. Wang, Z. Cheng, Z. Chen, J.-B. Xu, H. K. Tsang, and C. Shu, "Graphene photodetector integrated on silicon nitride waveguide," *Journal of Applied Physics*, vol. 117, no. 14, Article ID 144504, 2015.

[57] Z. Cheng, J. Wang, K. Xu, H. K. Tsang, and C. Shu, "Graphene on silicon-on-sapphire waveguide photodetectors," in *Graphene on silicon-on-sapphire waveguide photodetectors*, 2015, p. STh1I.5.

[58] M. Chhowalla, H. S. Shin, G. Eda, L.-J. Li, K. P. Loh, and H. Zhang, "The chemistry of two-dimensional layered transition metal dichalcogenide nanosheets," *Nature Chemistry*, vol. 5, no. 4, pp. 263–275, 2013.

[59] C. Zhi, Y. Bando, C. Tang, H. Kuwahara, and D. Golberg, "Large-scale fabrication of boron nitride nanosheets and their utilization in polymeric composites with improved thermal and mechanical properties," *Advanced Materials*, vol. 21, no. 28, pp. 2889–2893, 2009.

[60] H. Mu, S. Lin, Z. Wang et al., "Black phosphorus–polymer composites for pulsed lasers," *Advanced Optical Materials*, vol. 3, no. 10, pp. 1447–1453, 2015.